

Optimal Primary Frequency Regulation Control Strategy for Wind Farms to Prevent Secondary Frequency Drop

Kuiye Chen^{1, a}, Lu Miao^{1, b}, Deyang Chen^{1, c}, Yingjie Qin^{1, d},
Wenqing Jian^{2, e*}, and Kaiyue Duan^{2, f}

¹ System Analysis Department, Guangdong Power Grid Dispatching Control Center, Guangzhou, China;

² School of Electrical Engineering, South China University of Technology, Guangzhou, China.

^a chenkuiye@163.com, ^b miaolu@gddd.csg.cn, ^c chendy@csg.cn, ^d 451503825@qq.com, ^e 202321025094@mail.scut.edu.cn, ^f 202321015089@mail.scut.edu.cn

Abstract. As the share of wind power in the power generation structure increases, the demand for effective frequency regulation using wind turbines also grows. Wind turbines typically participate in frequency regulation by reducing rotor speed. However, extended operation at low speeds can lead to efficiency losses, which necessitate measures to disengage from frequency regulation. Additionally, actively disengaging wind turbines from frequency regulation may give rise to secondary frequency drop issues. To address this challenge, this paper proposes an optimized frequency regulation control strategy for wind turbines. Firstly, this paper analyzes traditional frequency regulation strategies and adjusts the parameters to address the issues of rapid energy release and frequency fluctuations in virtual inertia control. Secondly, an active disengagement strategy is introduced to reduce reliance on traditional frequency regulation parameters. Furthermore, the disengagement of droop control in frequency regulation is a key factor contributing to secondary frequency drops. In this paper, by adjusting the droop parameters, wind turbines can automatically disengage from frequency regulation in the later stages, thus preventing secondary frequency drops. Finally, simulation results show that integrating the adjusted parameters into comprehensive inertia control effectively demonstrates the validity of this approach.

Keywords: Primary frequency regulation of wind turbines; Secondary frequency drop; Frequency regulation parameter tuning; Active disengagement from frequency regulation.

1. Introduction

With the increasing share of renewable energy, the inertia level of power systems has significantly decreased. As a result, the risk of frequency instability after system disturbances has been exacerbated, which directly threatens the safe and stable operation of the grid[1]. In recent years, severe frequency security incidents have frequently occurred in power grids around the world. On September 19, 2015, the East China Grid Corporation experienced a bipolar DC blocking incident, causing the system frequency to rapidly drop to 49.56Hz within 12 seconds[2]. This indicates that rapid and effective frequency regulation measures[3] are crucial for ensuring the frequency stability of power systems with a high proportion of renewable energy[4].

In terms of wind turbine power reserve for frequency regulation, power reserves are pre-allocated by adjusting the pitch and utilizing overspeed, or by flexibly complementing the advantages and disadvantages of pitch control and overspeed[5]. The control method for wind turbine frequency regulation is switched based on the actual operating conditions. In the case of wind turbine rotor kinetic energy for frequency regulation, supplementary power loop (SPL) are designed, considering parameters such as coupled frequency[6], rotational speed[7], and time[8], to achieve the coupling of active power output from wind turbines with grid frequency, thereby responding to frequency fluctuations[9,10].

Overall, existing research predominantly focuses on wind turbines as the control object[11], designing frequency regulation strategies for single wind farms. However, with the increasing

installed capacity of wind turbines in the system, the demand for wind turbines to have primary frequency regulation capabilities is growing[12,13]. Yet, after wind turbines participate in system frequency regulation, secondary frequency drop issues may arise during the process of disengaging from frequency regulation. This paper addresses this issue by tuning the frequency regulation parameters of the wind turbine and introducing an active disengagement strategy. By adjusting the droop parameters, the wind turbine can automatically disengage from frequency regulation in the later stages, thereby preventing secondary frequency drops.

2. The frequency regulation control strategy for wind turbines

The energy of the wind turbine during normal operation is:

$$E_k = \frac{1}{2} J \omega_r^2$$

Where J is the mechanical inertia, and ω_r is the angular velocity[14].

In general, the inertia time is defined as:

$$H = \frac{E}{S} = \frac{J \omega_r^2}{2S}$$

In the equation: S is the rated apparent power.

2.1 Virtual Inertia Control

To make better use of wind energy resources, Doubly Fed Induction Generators (DFIG) should always operate in Maximum Power Point Tracking (MPPT) mode. However, this approach means that these generators are unable to provide additional power to participate in primary frequency regulation when grid frequency fluctuates. By integrating virtual inertia control into the existing wind turbine control strategies, DFIGs can gain the ability to contribute to primary frequency regulation. When grid load disturbances occur, leading to frequency fluctuations, the active power output of the wind turbines is affected:

$$P = \frac{dE_k}{dt}$$

$$P = J \omega \frac{d\omega}{dt}$$

As analyzed above, the inertia time constant of the wind turbine is:

$$H = \frac{J \omega_r^2}{2S}$$

$$P = \frac{2SH}{\omega_r^2} \omega \frac{d\omega}{dt}$$

Expressed in per unit value as:

$$\bar{P} = 2H \omega \frac{d\bar{\omega}}{dt}$$

Since the rotor speed of the wind turbine deviates very little from the rated speed under normal conditions ($\bar{\omega} = 1$), the equation can be approximated as:

$$\bar{P} = 2H \frac{d\bar{\omega}}{dt}$$

$$\Delta P_1 = 2H \frac{df}{dt} = -K_1 \frac{df}{dt}$$

Where, K1 is the inertia coefficient.

The application of virtual inertia control technology in Doubly Fed Induction Generators (DFIG) can suppress frequency fluctuations in the initial stage of grid frequency disturbances by adjusting active power output. However, its effect is relatively short-lived and is mainly a transient response. In addition, this control strategy increases active power output by reducing the rotor speed, but during the process of rotor speed recovery, it may cause a secondary frequency drop in the system.

The control block diagram of virtual inertia control is shown in Fig 1:

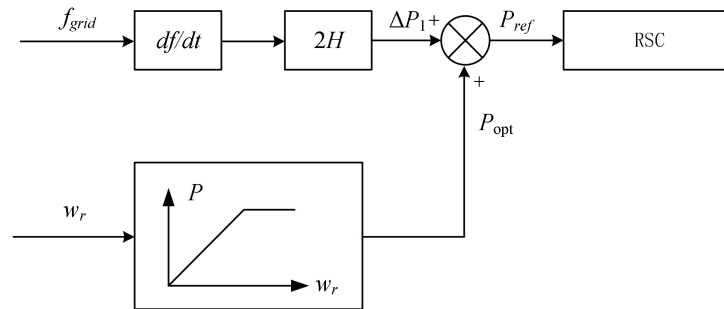


Fig. 1 The control block diagram of virtual inertia control

2.2 Droop control

When the grid frequency reaches its maximum or minimum point, the DFIG needs to assist in restoring the system to normal conditions through droop control. The purpose of droop control is to give the DFIG a frequency regulation function similar to that of a synchronous generator, enabling it to provide the necessary active power during the middle and later stages of frequency fluctuations. This helps maintain the balance of the grid frequency, and the process is a continuous and stable regulation mechanism.

$$\Delta P_2 = -K_2 \Delta f$$

Where K_2 is droop coefficient. And the control block diagram of droop control is shown in Fig 2 .

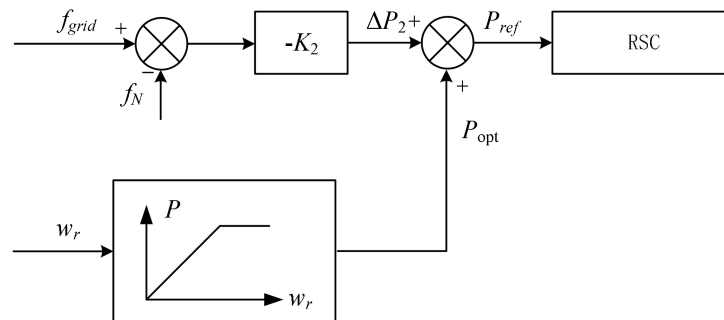


Fig. 2 The control block diagram of droop control

2.3 Comprehensive Inertia Control

The virtual inertia control technology ceases to output active power after the grid frequency reaches its minimum point, and instead starts absorbing energy from the grid. This results in its effectiveness being very limited, as it cannot provide effective support during the frequency recovery phase. In contrast, while the response of droop control is slower, it can increase active power output in proportion to the increase in frequency deviation. Therefore, when virtual inertia control stops providing active power, droop control continues to provide strong assistance. As a result, virtual inertia control is often combined with droop control, referred to as comprehensive inertia control. The formula for comprehensive inertia control is as follows:

$$\Delta P = -K_1 \frac{d\Delta f}{dt} - K_2 \Delta f$$

Where ΔP is the reference value for the active power in comprehensive inertia control.

The essence of comprehensive inertia control is still to use the system frequency as the input, and through the converter, release the kinetic energy stored in the rotor. This allows the originally decoupled DFIG to participate in frequency regulation, thereby enhancing the stability of the system. The block diagram of comprehensive inertia control is shown in Fig 3.

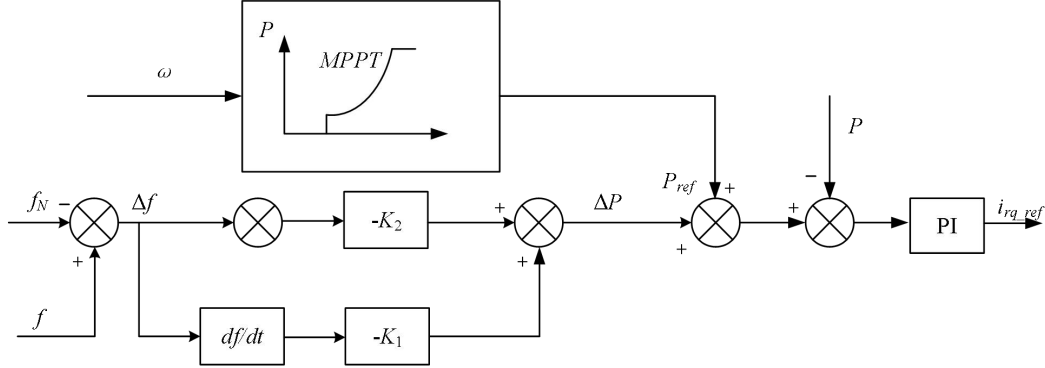


Fig. 3 Comprehensive Inertia Control Block Diagram

3. Tuning of Frequency Regulation Parameters for Wind Turbines

3.1 Tuning of Virtual Inertia Parameters

As previously mentioned, virtual inertia control varies with the rate of change of frequency, $d\Delta f/dt$, as shown in Fig 4. In the early stages of system frequency fluctuation, at time point t_0 , $d\Delta f/dt$ reaches its peak value. As the frequency regulation response of the power generation units gradually takes effect, the frequency drop is suppressed, and $d\Delta f/dt$ decreases accordingly. When the frequency reaches its minimum value, at time point t_1 , $d\Delta f/dt$ drops to zero. After this, the system frequency begins to rise, and $d\Delta f/dt$ becomes positive, continuing until the system reaches a new steady state, at which point $d\Delta f/dt$ returns to zero again.

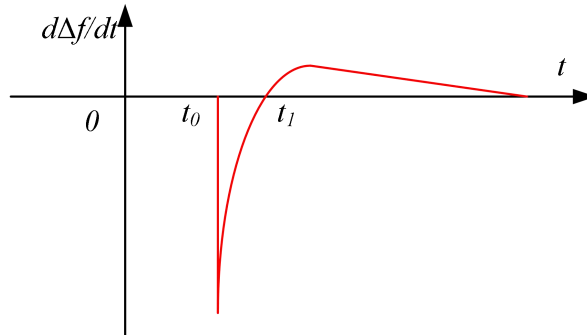


Fig. 4 Variation curve of $d\Delta f/dt$

The output of virtual inertia control will sharply rise from zero to the peak value at the initial moment. This abrupt change can cause the rotor speed to drop sharply in the early stage of frequency regulation, quickly releasing the rotor's kinetic energy. To avoid this situation, a first-order inertia link can be introduced before the parameter K_1 to achieve a gradual release of energy. The modified virtual inertia control parameter K_3 can be expressed as:

$$K_3 = \frac{T}{T_s + 1} K_1 \quad (2.1)$$

$$\Delta P_1 = -K_3 \frac{d\Delta f}{dt} = -K_1 \frac{T_s}{T_s + 1} \Delta f \quad (2.2)$$

From Fig 4, it can be observed that after the time point t_1 corresponding to the lowest frequency point, $d\Delta f/dt$ becomes positive. At this moment, the virtual inertia control of the DFIG starts to

absorb energy from the grid, which may lead to further frequency fluctuations. Therefore, adjusting parameter K_1 after $d\Delta f/dt$ becomes positive is necessary.

If K_1 is directly set to a negative value after $d\Delta f/dt$ becomes positive, it may cause frequency fluctuations in the system, as shown in Fig 5. To avoid this, a feasible approach is to set K_1 to zero after $d\Delta f/dt$ becomes positive. This adjustment can prevent the virtual inertia control from absorbing energy from the grid, thereby reducing the negative impact on the system's frequency stability.

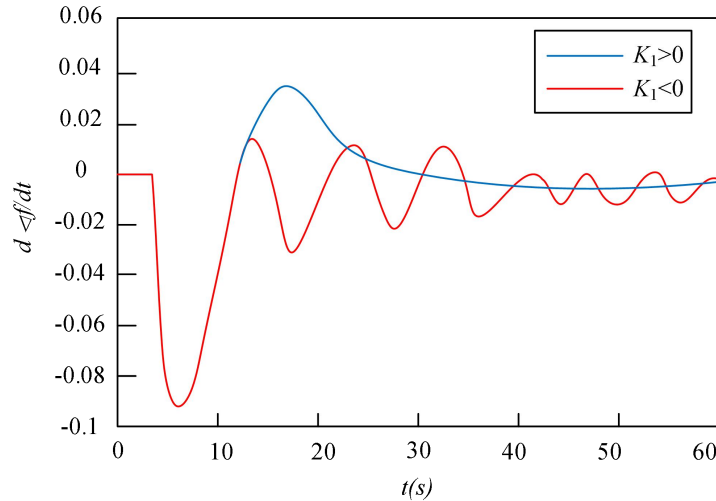


Fig. 5 The change curve of $d\Delta f/dt$ when K_1 takes positive or negative values.

In summary, when $d\Delta f/dt$ is less than 0, a first-order inertia link is added before parameter K_1 . When $d\Delta f/dt$ is greater than or equal to 0, parameter K_1 is directly set to 0. Therefore, the new parameter K_3 is:

$$K_3 = \begin{cases} \frac{T}{T_s + 1} K_1, & d\Delta f / dt < 0 \\ 0, & d\Delta f / dt \geq 0 \end{cases}$$

$$\Delta P_1 = \begin{cases} -K_1 \frac{T_s}{T_s + 1} \Delta f, & d\Delta f / dt < 0 \\ 0, & d\Delta f / dt \geq 0 \end{cases}$$

It can be seen that the improved virtual inertia control of the DFIG, after a sudden frequency change in the wind turbine, first outputs active power in response to the rate of frequency change. Once the frequency change rate is detected to be greater than zero, the virtual inertia power output is stopped to prevent the DFIG from absorbing energy from the system.

3.2 Tuning of Droop Parameters

In the frequency recovery stage of the power system, the effect of virtual inertia control gradually diminishes and tends to zero. At this point, the wind turbine exits frequency regulation, and the secondary frequency drop in the system is primarily caused by droop control. The principle of droop control indicates that when the system frequency reaches a steady state, there will be a certain deviation from the reference frequency f_{ref} . In this situation, the wind turbine will continue to provide frequency regulation power, causing the rotor to remain at low speeds. To ensure the safety of the turbine, it is necessary to prevent the rotor from staying at low speeds for extended periods. Therefore, once the system frequency reaches a steady state, the turbine will disengage from frequency regulation. However, the turbine's disengagement from frequency regulation results in a sudden reduction in system frequency regulation power, leading to a secondary frequency drop, as shown in Fig 6, where t_{off} represents the time when the turbine exits frequency regulation.

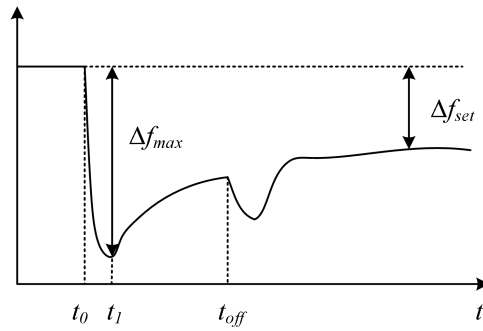


Fig. 6 Frequency variation after wind turbine droop control exits frequency regulation

As shown in Fig 6, after experiencing the lowest frequency point t_1 during the frequency adjustment, in order to prevent further frequency decline, the droop control output of the wind turbine needs to gradually decrease. This can be achieved by adjusting the fixed parameter K_2 to reduce it progressively. In the initial stage, this parameter should remain at the initial value of 1, and then gradually decrease after the frequency reaches its lowest point, approaching zero. To achieve this, the Logistic function is ultimately chosen. The Logistic function smoothly transitions from the initial value f_0 to 1, changing slowly at first, then rapidly declining, and slowing down again as it approaches 1. The expression of the function is as follows:

$$f(t) = \frac{f_0 e^{rt}}{1 + f_0 (e^{rt} - 1)}$$

To transform the function $f(t)$ so that it decreases from 1 to f_0 , the resulting function $F(t)$ is as follows:

$$F(t) = 1 + f_0 - \frac{f_0 e^{rt}}{1 + f_0 (e^{rt} - 1)}$$

It can be seen that the values of f_0 and the rate of change r affect the time it takes for the function $F(t)$ to decrease from 1 to f_0 .

When the initial frequency f_0 is held constant, a decrease in the parameter r will result in an increase in the time required for the function $F(t)$ to reach f_0 . Similarly, if r remains unchanged but f_0 is decreased, the time for $F(t)$ to decrease to f_0 will also be extended. Therefore, selecting appropriate values for f_0 and r is crucial. In this study, we chose $r = 6/15$ and $f_0 = 0.001$. The corresponding graph of the function $F(t)$ is shown below:

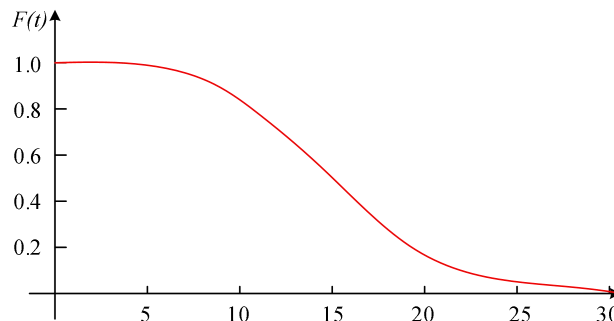


Fig. 7 $F(t)$ Value Change Curve

According to the data shown in Fig 7, before 10 seconds, the function $F(t)$ remains close to its initial value. When the system experiences frequency changes, the lowest point of the frequency typically occurs within 5 seconds, meaning that during this time, the DFIG does not reduce its frequency regulation output. Between 10 and 25 seconds, the function $F(t)$ drops rapidly, and it approaches zero around 30 seconds, marking the point where the DFIG exits the frequency

regulation process. Throughout this time variation, $F(t)$ does not show any extremum points, indicating that the reduction in the droop output of the DFIG does not cause frequency fluctuations. The new parameter K_4 in the droop control is set as follows:

$$K_4 = \left(1 + f_0 - \frac{f_0 e^{\tau}}{1 + f_0 (e^{\tau} - 1)} \right) K_2$$

The droop control power of the wind turbine after parameter improvement is:

$$\Delta P_2 = -K_4 \Delta f$$

In the initial stage of frequency regulation, the DFIG uses the improved virtual inertia control and droop control to jointly provide active power to suppress frequency fluctuations in the system. As the system frequency recovers, and as ΔP_1 gradually approaches zero, the improved virtual inertia control will gradually disengage from the frequency regulation process. Meanwhile, the output ΔP_2 provided by droop control will also gradually decrease over time after the frequency reaches its minimum point, eventually disengaging from frequency regulation automatically. The active power change ΔP of the DFIG during the frequency regulation process is expressed as:

$$\Delta P = -(K_3 + K_4) \Delta f$$

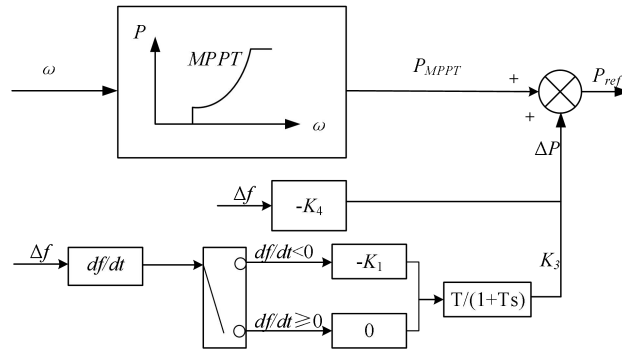


Fig. 8 Improved Parameterized Comprehensive Inertia Control

4. Active Disengagement Frequency Regulation Strategy for Wind Turbines

Based on the previous analysis, we can conclude that when the frequency rate of change, $d\Delta f/dt$, is greater than or equal to zero, the value of K_3 becomes zero, indicating that the virtual inertia control has completed its role in the primary frequency regulation process. After improving the parameter K_3 , we introduce the time constant T , as different values of T will affect the timing of DFIG's disengagement from virtual inertia control. To simplify the calculation, we further simplify the previous SFR model, considering the system as consisting of synchronous generators, wind turbines, and loads, where the output of the synchronous generator is simplified into a droop control form. At a certain moment, the system encounters a sudden load increase ΔP_D , as shown in Fig 9.

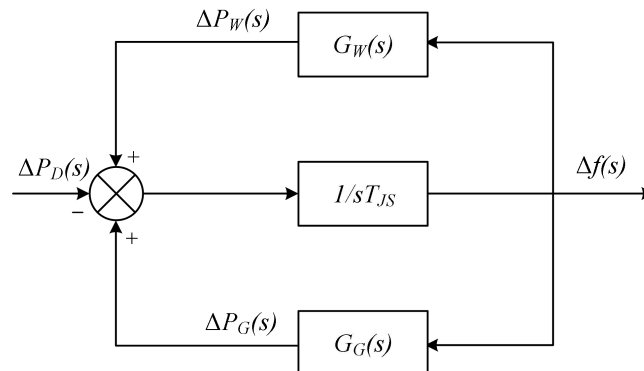


Fig. 9 Simplified SFR model with wind power integration

Frequency deviation $\Delta f(s)$:

$$\Delta f(s) = \frac{1}{sT_J} (\Delta P_G(s) + \Delta P_w(s) - \Delta P_D(s))$$

In the formula, T_J represents the inertia time constant of the synchronous generator.

For the synchronous generator, the frequency regulation power increment ΔP_G is:

$$\Delta P_G(s) = -K_G \Delta f$$

In the formula, K_G is the frequency regulation coefficient of the synchronous generator. For the wind turbine, its frequency regulation power increment ΔP_W is:

$$\Delta P_w(s) = -\frac{K_1 T_s}{1 + T_s} \Delta f$$

$$\Delta P_w(s) = \frac{K_1 \Delta P_D}{T_J} \frac{1}{s^2 + 2\xi \omega_n s + \omega_n^2}$$

In the formula, $\left\{ \begin{array}{l} \omega_n = \sqrt{\frac{K_G}{T_J T_G}} \\ \xi = \left(\frac{T_J + K_G T + K_1 T}{2K_G} \right) \omega_n \end{array} \right.$.

The inverse Laplace transform of the equation gives the power output ΔP_W of the wind turbine as:

$$\Delta P_w = \frac{K_1 \Delta P_D}{T_J \sqrt{1 - \xi^2} \omega_n} e^{-\xi \omega_n t} \sin\left(\sqrt{1 - \xi^2} \omega_n t\right)$$

Taking the derivative of the formula and setting the derivative equal to zero, the maximum value of ΔP_W can be obtained as:

$$\Delta P_{w \max} = \frac{K_1 \Delta P_D}{T_J \sqrt{1 - \xi^2} \omega_n} e^{\frac{-r\xi}{\sqrt{1 - \xi^2}}} \sin r$$

In the formula, $r = \arctan \frac{\sqrt{1 - \xi^2}}{\xi}$.

Setting $\Delta P_W = 0$, the frequency regulation disengagement time t_{off_under} DFIG virtual inertia control can be obtained as:

$$t_{off} = \frac{\pi}{\sqrt{1 - \xi^2} \omega_n}$$

In summary, as the time constant T increases, the output power under DFIG virtual inertia control increases. However, the frequency regulation disengagement time also becomes longer. Therefore, a reasonable selection of the time constant T is required.

5. Simulation

5.1 Comparison of Frequency Regulation Performance with Improved Virtual Inertia Control Parameters and Rotor Speed Recovery

5.1.1 Comparison of Parameter K_3 and Parameter K_I without Active Disengagement from Frequency Regulation

At 10 seconds, the switch for the load of 5 MW is turned on, resulting in a sudden increase of 20 MW in system load. The simulation time is 70 seconds, and the system's rated frequency is 50 Hz.

The improved parameter K_3 with different T values (where K_3 does not actively disengage from frequency regulation after the frequency rate of change exceeds zero) is compared with the traditional virtual inertia control parameter K_1 .

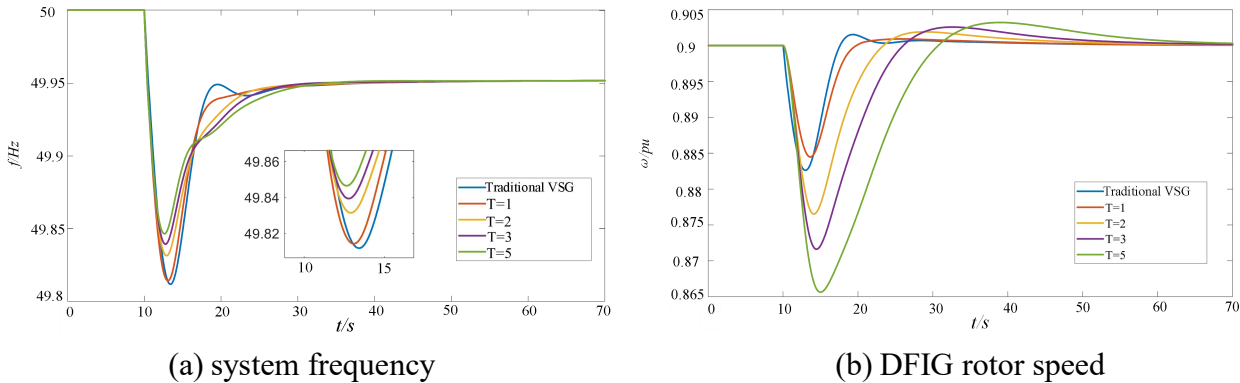


Fig. 10 Simulation curves of wind turbine participation in frequency regulation under different values of parameter K_3 and time constant T

Fig 10(a) shows that traditional virtual inertia control causes a secondary frequency drop. When T is set to 5, the lowest frequency point improves compared to traditional control, but the rotor speed decreases more significantly. This is because the improved K_3 parameter allows the wind turbine's rotor energy to participate more effectively in frequency regulation. As the value of T increases, the lowest frequency rises, the maximum deviation decreases, and the time to reach the lowest point shortens, thereby improving the frequency more effectively.

Fig 10(b) shows that during the rotor speed recovery phase, the rotor speed exceeds the initial value. This is because when $d\Delta f/dt$ is positive, the DFIG absorbs energy from the grid. As $d\Delta f/dt$ approaches zero, the rotor speed gradually returns to its initial value, requiring the wind turbine to actively disengage from frequency regulation. The increase in T results in a longer recovery time for the rotor speed to stabilize, because a larger T value means the turbine releases more energy, causing the rotor speed to drop, and thus the recovery time increases.

5.1.2 Comparison of Improved Parameter K_3 with and without Active Disengagement of Frequency Regulation under the Same T Value

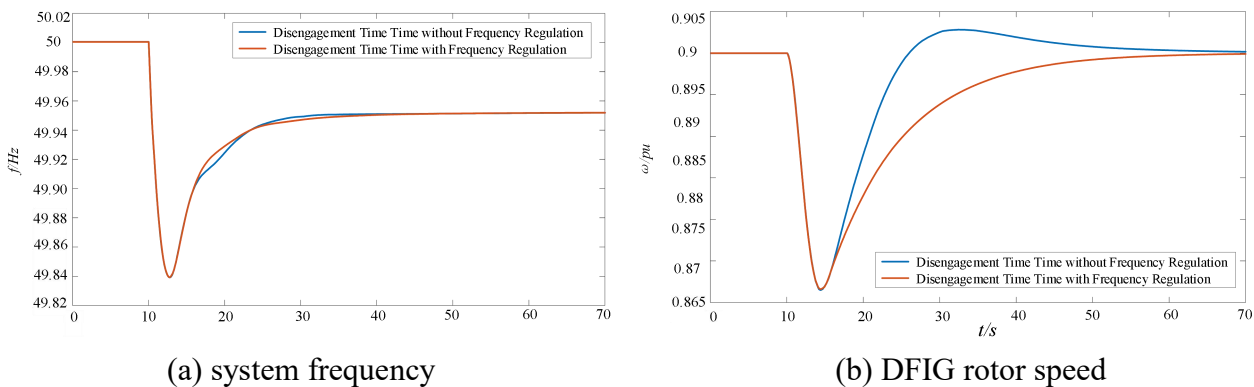


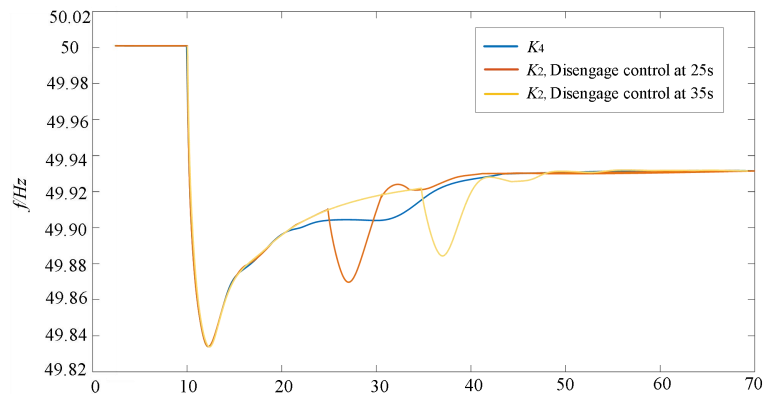
Fig. 11 The frequency regulation simulation curve of DFIG with and without disengagement under the improved parameter K_3 when $T=3$

As shown in Fig 11, under the improved parameter K_3 , after actively disengaging from frequency regulation, the DFIG rotor speed does not exceed the initial speed during the recovery process, and the system frequency recovers without fluctuation. This is because, after disengaging from frequency regulation, the DFIG does not absorb power from the grid for rotor speed recovery but instead relies on its own mechanical power to recover the rotor speed.

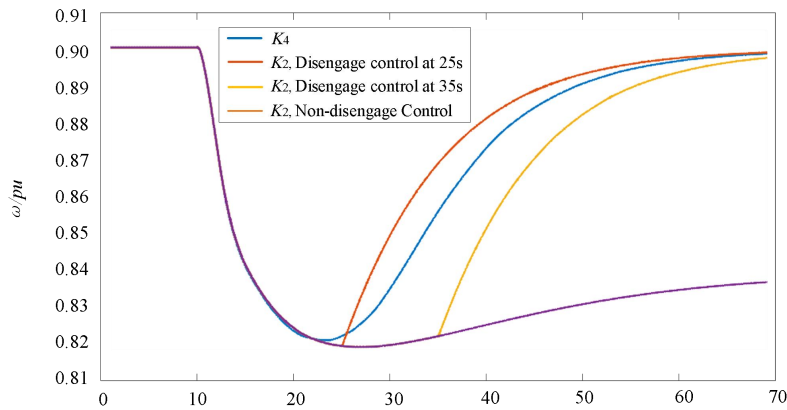
5.2 Comparison of Frequency Regulation Effect and Rotor Speed Recovery After Droop Control Parameter Improvement

In the frequency regulation control of the DFIG, the virtual inertia control uses the improved parameter K_3 , while the droop control uses the traditional parameter K_2 and the improved parameter K_4 , respectively. Under the improved parameter K_4 , the wind turbine naturally disengages from frequency regulation, while under the traditional parameter K_2 , the wind turbine disengages at 25s and 35s, with the same frequency regulation coefficient in both cases.

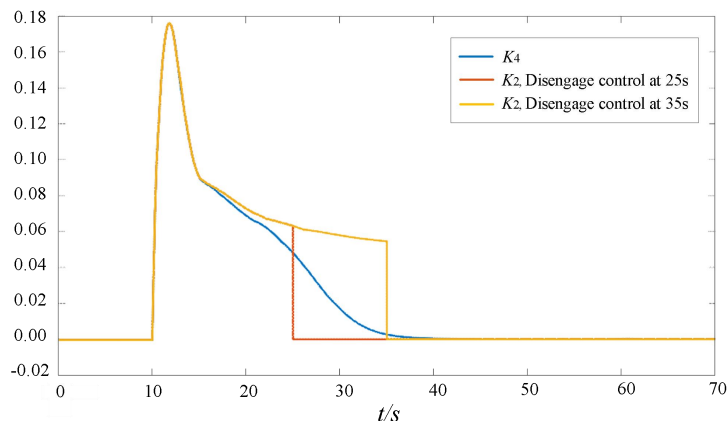
To verify the effectiveness of the improved parameter K_4 for the DFIG, and to confirm its continued validity even after increasing the wind turbine penetration, the following simulation is conducted: 35 wind turbines with a penetration rate of 20.79%.



(a) system frequency



(b) DFIG rotor speed



(c) DFIG frequency regulation power

Fig. 12 The frequency regulation simulation curve under droop control with improved parameter

From Fig 12(a), it can be seen that after the wind turbine passes the frequency minimum point with the traditional parameter K2, the timing of disengagement from frequency regulation does not affect the magnitude of the secondary frequency drop, indicating that simply adjusting the disengagement time is not sufficient. Additionally, after the wind turbine disengages from frequency regulation, the frequency recovery process still shows secondary fluctuations, so improvements to the traditional parameters are needed.

When the improved parameter K4, is adopted, the minimum frequency value remains almost unchanged, indicating that the improved droop control parameter meets the design requirements during the early stage of frequency regulation without reducing power output. From Fig 12 (c), it can be seen that throughout the entire power reduction process, no secondary frequency drop occurs. From Fig 12 (b), it is evident that with the traditional parameter K2, if the wind turbine does not disengage from frequency regulation, the rotor speed remains low continuously.

After adopting the improved parameter K4, the rotor speed begins to recover around 25 seconds, whereas under the traditional parameter K2, the speed starts to recover only after disengaging from frequency regulation. At the end of the simulation, at 35 seconds, the rotor speed under the traditional parameter K2 has not yet returned to its initial value, indicating that the later the disengagement time, the longer it takes for the rotor speed to recover to its initial value. In contrast, with the improved parameter K4, the system does not need to actively control the disengagement time for the wind turbine to recover speed; the wind turbine automatically restores its speed to the initial value.

6. Conclusion

With the deepening of research on wind turbine frequency regulation capabilities, the issue of secondary frequency drops when the wind turbine disengages from frequency regulation has become increasingly prominent. To avoid secondary frequency drops, this paper fine-tunes the frequency regulation parameters for the DFIG. The main work and conclusions are as follows:

(1) Optimization of DFIG Virtual Inertia Control Parameter K2:

The virtual inertia control parameter K1 is optimized by introducing a first-order inertia element and setting K1 to zero when $d\Delta f/dt$ is positive, forming the new parameter K3. Simulation results show that the improved K3 significantly enhances the minimum frequency and promotes rotor speed recovery. Additionally, the value of T in K3 has a significant impact on the minimum frequency and frequency regulation disengagement time. An increase in T improves the minimum frequency but leads to a more noticeable decrease in rotor speed, releasing more energy and thus prolonging the rotor speed recovery time.

(2) Adjustment of DFIG Droop Control Parameter K2:

The droop control parameter K2 is adjusted by introducing a Logistic function, which maintains power output in the early stage of frequency regulation and gradually reduces power in the later stage, avoiding a sudden drop in power that could cause a secondary frequency drop. Simulation validation shows that the DFIG using the improved K3 parameter does not lead to secondary frequency drops and effectively manages frequency regulation, ensuring system stability after disengagement.

Acknowledgements

This research was funded by Science and technology projects of China Southern Power Grid Corporation No. 036000KK52222013(GDKJXM20222142).

References

- [1] ON E, NETZ G, Grid connection regulations for high and extra high voltage[R]. Bayreuth: E. ON Netz GmbH, 2006.

- [2] Ding H, Miao Y, Huang Z, et al. Test and analysis of renewable-energy active frequency support capability of East China Power Grid[C]. 2022 Power System and Green Energy Conference (PSGEC), 2022: 196-201.
- [3] WU Z P, GAO W Z, GAO T Q, et al. State-of-the-art review on frequency response of wind power plants in power systems[J]. Journal of Modern Power Systems and Clean Energy, 2018, 6(1) : 1-16.
- [4] CHENG Y, AZIZIPANAH-ABARGHOOEE R, AZIZI S, et al. Smart frequency control in low inertia energy systems based on frequency response techniques: a review[J]. Applied Energy, 2020, 279: 115798.
- [5] GAO D W, WU Z P, YAN W H, et al. Comprehensive frequency regulation scheme for permanent magnet synchronous generator-based wind turbine generation system[J]. IET Renewable Power Generation, 2019, 13(2): 234-244.
- [6] MORREN J, DE HAAN S W H, KLING W L, et al. Wind turbines emulating inertia and supporting primary frequency control[J]. IEEE Transactions on Power Systems, 2006, 21(1): 433-434.
- [7] HWANG M, MULJADI E, JANG G, et al. Disturbanceadaptive short-term frequency support of a DFIG associated with the variable gain based on the ROCOF and rotor speed[J]. IEEE Transactions on Power Systems, 2017, 32(3): 1873-1881.
- [8] YANG D J, GAO H C, ZHANG L, et al. Short-term frequency support of a doubly-fed induction generator based on an adaptive power reference function[J]. International Journal of Electrical Power&Energy Systems, 2020, 119: 105955.
- [9] BAO W Y, DING L, LIU Z F, et al. Analytically derived fixed termination time for stepwise inertial control of wind turbines: Part I analytical derivation[J]. International Journal of Electrical Power&Energy Systems, 2020, 121: 106120.
- [10] GUO Y C, BAO W Y, DING L, et al. Analytically derived fixed termination time for stepwise inertial control of wind turbines: Part II application strategy[J]. International Journal of Electrical Power&Energy Systems, 2020, 121: 106106.
- [11] Chen S, Fang X, Zhang M, et al. Frequency Modulation Strategy Based on Hierarchical Coordinated Control of Wind Power, Thermal Power and Energy Storage[C].2023IEEE6th International Electrical and Energy Conference(CIEEC), 2023: 2878-2883
- [12] Yan X, Sun X. Inertia and droop frequency control strategy of doubly-fed induction generator based on rotor kinetic energy and supercapacitor[J]. Energies, 2020, 13(14): 3697.
- [13] Lingang Y, Xiaohe W, Zhaohui W, et al. Research on control strategy of virtual synchronous generator based on energy storage wind farm[C].2021IEEE5th Advanced Information Technology, Electronic and Automation Control Conference(IAEAC), 2021: 240-244
- [14] Ma Y, Yu P. Research on Combined Frequency Regulation Control Method of Wind Storage with Storage System Optimized Intervals Considered[J]. Mathematical Problems in Engineering, 2022, 2022: 6872799.
- [15] Wang X, Ye X, Wei W, et al. The Frequency Control Strategy of a Wind-Storage Combined System Considering Battery SOC[J]. Electronics, 2023, 12(16): 3453.